電気学会論文誌 A（基礎・材料・共通部門誌）
IEEJ Transactions on Fundamentals and Materials
Vol.139 No.2 pp.92-98 DOI: 10.1541/ieejfms.139.92

Paper

Molecular Dynamics Simulation and Quantum Chemical Calculations of Surfactant Having Suppression Effect on Water Trees

Hiroaki Uehara[*a)] Member, Shinya Iwata[**] Member
Yasuo Sekii[***] Life Member, Tatsuo Takada[*4] Life Member
Yang Cao[*5] Non-member

(Manuscript received April 29, 2018, revised Nov. 16, 2018)

Polyethylene (PE) is a hydrophobic polymeric insulating material. It has been found that adding hydrophilic additives can enhance the water tree resistance of PE. Such additives are most often surfactants that contain both hydrophobic and hydrophilic groups within their molecular structures. It is considered that a surfactant added to PE surrounds water molecules and stabilizes them. Hence, it is highly plausible that the solubilization of moisture in a supersaturated state leads to the suppression of water tree initiation in PE. In this study, we investigated the aggregation of water molecules and the orientation of surfactants toward water clusters by molecular dynamics (MD) simulation. In addition, quantum chemical calculations were performed to reveal the mechanism by which a surfactant suppresses water tree initiation. A comparison of the computational results with experiments suggests that the addition of a surfactant is extremely effective in suppressing bow-tie water trees.

Keywords : molecular dynamics simulation, quantum chemical calculation, polyethylene, surfactant, suppression effect, water tree

1. Introduction

Water treeing occurs when an electric field is applied to an insulating material in contact with water[(1)]. Water trees occur at the interface between the insulating layer and an electrode, void, or contaminant in the insulating material. Polyethylene (PE), used widely as an insulating material for power cables, is a hydrophobic polymeric insulating material. On the other hand, a surfactant contains both hydrophobic and hydrophilic groups in its molecular structure. It is considered that a surfactant added to PE surrounds water molecules and stabilizes them. Sekii, et al. experimentally revealed that hydrophilic additives can enhance the water tree resistance of PE[(2)(3)]. They also confirmed that the addition of a surfactant suppresses bow-tie water trees (BTTs)[(2)(3)]. Molecular dynamics (MD) simulations have been conducted for systems including polymers and water molecules[(4)-(8)]. However, few studies have been conducted on the suppression effect of water trees by performing MD simulations and quantum chemical calculations[(9)].

In this study, we investigated the aggregation of water molecules and the orientation of surfactants toward water clusters in PE chains by MD simulation. Furthermore, quantum chemical calculations were performed for the case of a surfactant in proximity to a small water cluster with reference to experimental results.

a) Correspondence to: Hiroaki Uehara. E-mail: huehara@kanto-gakuin.ac.jp
* Kanto Gakuin University
1-50-1, Mutsuura-higashi, Kanazawa-ku, Yokohama 236-8501, Japan
** Osaka Research Institute of Industrial Science and Technology
2-7-1, Ayumino, Izumi, Osaka 594-1157, Japan
*** Sekii PE Laboratory
1-18-28-817, Chuoh-koh, Chuoh-ku, Chiba 260-0024, Japan
*4 Tokyo City University
1-28-1, Tamazutsumi, Setagaya-ku, Tokyo 158-8557, Japan
*5 University of Connecticut
97, North Eagleville Road, Storrs, CT 06269-3136, USA

2. Simulation Method

2.1 PE and Surfactant Figure 1 shows the molecular structure of PE and the surfactant considered in this study[(2)(3)]. We used PE as a base material, as shown in Fig. 1 (a). We also used an amphiphilic surfactant having both a hydrophobic group and a hydrophilic group in its molecular structure, as shown in Fig. 1 (b).

In a surfactant, the hydrophobic group is a nonpolar group with strong affinity to oil and low affinity to water. The hydrophobicity increases if there are many hydrocarbon chains such as alkyl groups or cyclic structures such as aryl groups. In contrary, the hydrophilic group has a large polarity and strong affinity to water. The hydrophilic group forms weak bonds with water molecules by electrostatic action or hydrogen bonding. Representative hydrophilic groups are the hydroxyl group, amino group, and carboxyl group.

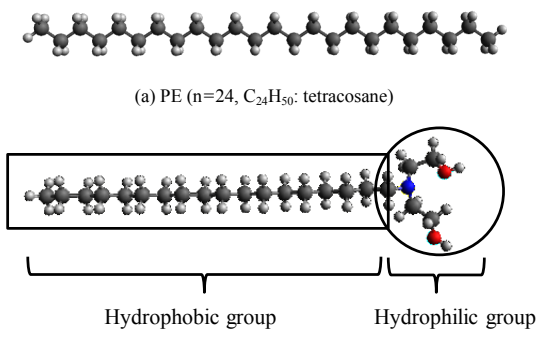

(a) PE (n=24, $C_{24}H_{50}$: tetracosane)

(b) Surfactant ($C_{22}H_{47}NO_2$: Stearyldiethanolamine)

Fig. 1. Molecular structure of PE and surfactant

When surfactants are added to hydrophobic polymers such as cross-linked polyethylene (XLPE), water molecules aggregate to form water clusters, and the surfactants and water clusters in XLPE are considered to form micelles in the amorphous region of the XLPE in the presence of water, as shown in Fig. 2[(2)(3)]. Such micelle structures comprising a water cluster surrounded by surfactants are thermodynamically stable. Hence, it is highly plausible that the solubilization of moisture in the supersaturated state will lead to the suppression of water tree initiation in XLPE.

2.2 Reference Experimental Results Figure 3 shows the volume density of BTTs in XLPE with and without surfactants obtained by Sekii and co-workers[(2)(3)]. We can clearly see that the volume density of BTTs in the case with surfactants is smaller than that without surfactants. Therefore, it is considered that the surfactants suppress BTT initiation.

2.3 Quantum Chemical Calculations In this study, we used the Gaussian 09 quantum chemical program to obtain the electric dipole moments, energy levels, molecular orbitals, and three-dimensional (3D) electrostatic potential distributions of the PE, surfactants, water molecules, water clusters, and combined water clusters and surfactants[(10)]. More specifically, we applied B3LYP as the exchange-correlation functional and 6-31g* as the basis set[(11)(12)]. High-precision second-order Møller–Plesset perturbation theory (MP2), an improvement over the Hartree–Fock (HF) ab initio method[(13)(14)], is often used for quantum chemical calculations of water molecules or water clusters. However, its practicality strongly depends on the performance of the computer and can be time demanding. Therefore, we used density functional theory (DFT) to perform highly accurate calculations in a relatively short time.

2.4 MD Simulation MD simulation is used to investigate the physical motion of atoms and molecules[(4)-(9)]. First, the initial arrangement of atoms or molecules is determined. After that, the forces exerted by one atom or molecule on another are calculated. The forces acting between atoms or molecules comprise the chemical bonding forces when atoms form molecules, the electrostatic forces generated by positively or negatively charging atoms or molecules, and the intermolecular forces acting between molecules. Then, these forces are summed. Next, the motion of atoms or molecules subjected to these forces is calculated in accordance with Newton's laws of motion. This reveals how the arrangement of atoms or molecules has changed from the initial arrangement after a certain time.

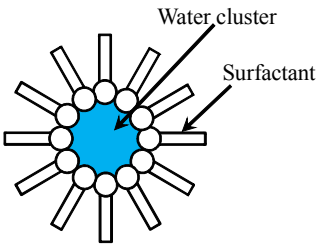

Fig. 2. Micelle formed in amorphous region of XLPE

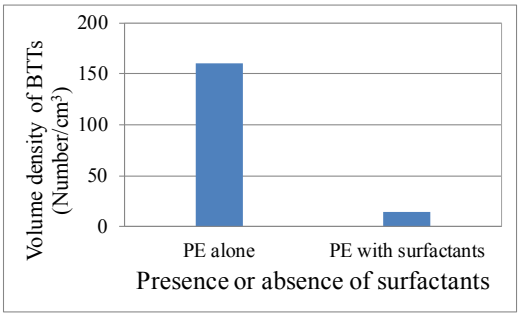

Fig. 3. Volume density of BTTs in XLPE with and without surfactants[(2)(3)]

In this study, we used Gromacs 5.0.7 as the software for MD simulation to determine the molecular structure and to clarify the effect on the diffusion and aggregation of PE, the surfactant, and water molecules. Here, the four-point transferable intermolecular potential (TIP4P) was used for the water molecules[(15)]. TIP4P improves the electrostatic distribution around the water molecules by slightly shifting the charge of the oxygen atom toward the hydrogen atom.

The general Amber force field[(16)] (GAFF) and 3D periodic boundary conditions were employed in the x, y, and z directions. Furthermore, the Lennard–Jones potential was used to approximate the interaction between the combination of neutral atoms or molecules in this simulation. The particle-mesh Ewald (PME) summation was used for the Coulombic interaction[(17)]. All bonds including hydrogen were employed using a linear constraint solver (LINCS) algorithm[(18)]. A fixed time step of 2 fs was used throughout all MD simulations.

The procedure of the MD simulation was as follows. First, PEs, surfactants, and water molecules were randomly arranged in a cell. After that, the energy of the cell was minimized using the method of steepest descent. In this steepest descent method, the energy minimization calculation is terminated when the system becomes 100 kJ mol^{-1} nm^{-1} or less. Next, an NVT ensemble with a constant volume and constant temperature of 300 K, controlled by a Nosé–Hoover thermostat[(19)(20)], was applied to the system for 250,000 steps (500 ps). Then, an NPT ensemble with a constant temperature of 300 K and a constant pressure of 100 kPa, controlled by the Parrinello–Rahman barostat[(21)], was conducted for 5,000,000 steps (10 ns). Finally, an NPT production run under the same conditions as the NPT ensemble was conducted for 5,000,000 steps (10 ns). During the production run, the molecular trajectory was recorded every 1,000 steps.

3. Results and Discussion

3.1 Aggregation of Water Molecules and Orientation of Surfactant toward Water Cluster by MD Simulation Figure 4 shows the initial structure, final structure, and an enlarged view of the final structure near a water cluster for each MD simulation model, whose parameters are summarized in Table 1. To emphasize the water molecules and surfactants, the PE molecules in Fig. 4 are indicated by wire-type structures. It can be seen that the water molecules aggregate and form a water cluster. Moreover, the hydrophilic groups of surfactants are oriented toward the water cluster in PE chains, as shown in Figs. 4 (b) and (c). Figure 5 shows the density of PE chains as a function of time during the 10 ns NPT production run for each model. These values are in good agreement with the literature[(4)(5)(22)].

Here, we used the radial distribution function (RDF) to analyze the structure of the formed water cluster. The RDF in a system of atoms or molecules describes how the density varies as a function of distance from a reference atom or molecule. The RDF of water molecules was calculated from the molecular trajectory obtained during the 10 ns NPT production run.

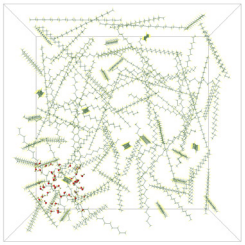

Initial structure

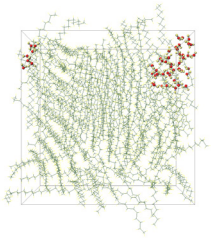

Final structure

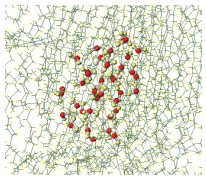

Enlarged view near water cluster

(a) Model A

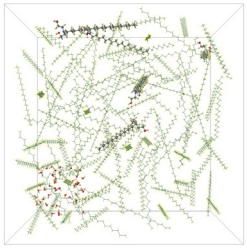

Initial structure

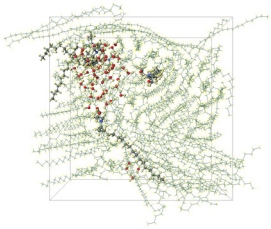

Final structure

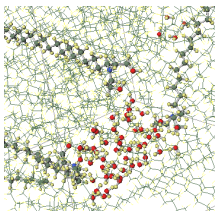

Enlarged view near water cluster

(b) Model B

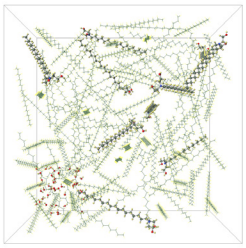

Initial structure

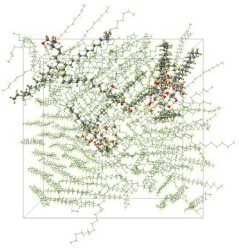

Final structure

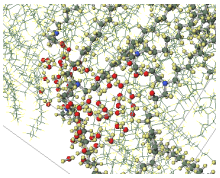

Enlarged view near water cluster

(c) Model C

Fig. 4. Initial structure, final structure, and enlarged view of final structure near water cluster for each MD simulation model

Table 1. Parameters of MD simulation models

Model	A	B	C
Number of PEs	100	100	100
Number of surfactants	0	5	10
Number of water molecules	50	50	50
wt% of PEs	97.4	92.6	88.3
wt% of surfactants	0	4.9	9.3
wt% of water molecules	2.6	2.5	2.4
Density of initial structure (kg/m^3)	200	200	200
Density of final structure (kg/m^3)	872	847	862

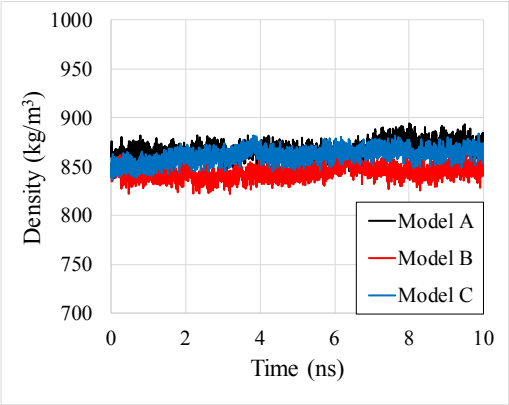

Fig. 5. Density of PE chains as a function of time during 10 ns NPT production run for each model

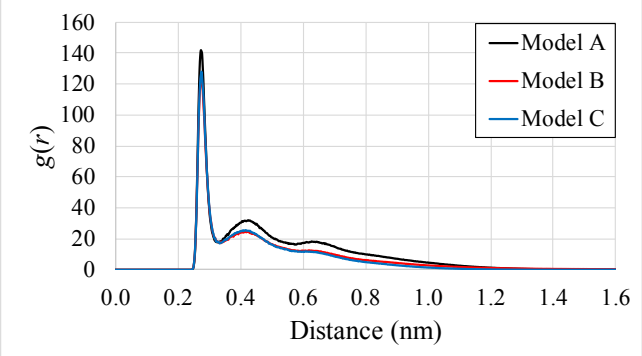

Fig. 6. RDF between oxygen atoms of water molecules for each MD simulation model

Figure 6 shows the RDF between the oxygen atoms of water molecules for each MD simulation model. Here, $g(r)$ is the probability that another oxygen atom of a water molecule exists at a distance r from the reference oxygen atom of a water molecule. At distance r from the reference oxygen atom, with the number of oxygen atoms between two spherical shells with radii r and $r+dr$ represented as $n(r)$, the density of oxygen atoms in the spherical shell is

$$\frac{n(r)}{4\pi r^2 dr} \quad \cdots\cdots (1)$$

Dividing Eq. (1) by the average density ρ of the system yields the RDF $g_i(r)$ of oxygen atom i.

$$g_i(r) = \frac{n(r)}{4\pi r^2 dr \rho} \quad \cdots\cdots (2)$$

The average of Eq. (2) is taken as the RDF $g(r)$ of the system.

$$g(r) = < g_i(r) > = \frac{< n(r) >}{4\pi r^2 dr \rho} \quad \cdots\cdots (3)$$

In Fig. 6, the first sharp peak is at 0.28 nm and the second broad peak is at 0.42 nm. Although the value of $g(r)$ is zero at 0.24 nm or less, this means that the oxygen atoms of water molecules do not overlap each other. The first sharp peak at 0.28 nm indicates the high probability of oxygen occupancy of adjacent water molecules[4][9][23-25]. Since the distance between adjacent oxygen atoms exhibiting hydrogen bonding between is 0.272 nm, the sharp peak is considered to correspond to the interaction due to hydrogen bonding. The second broad peak at 0.42 nm represents the distance to second-neighbor oxygen atoms.

Since whole pairs between oxygen atoms of water molecules are averaged and divided by the density as shown in Eqs. (1) to (3), $g(r)$ is considered that there is no contradiction even if it becomes extremely large. Although the RDF is originally used to describe the structure of clusters and liquid containing water, we focused on the distance between oxygen atoms in water molecules instead of clusters in this MD simulation.

On the other hand, it is difficult for the whole system after MD simulation to distinguish between crystalline and amorphous. It is also difficult to consider from the gauche-trans (anti) conformation in terms of current PE length, the number of PE molecules and the calculation time[22][26][27]. The influence of the structure determined by the initially placed molecular position and subsequent NVT ensemble should remain in the production run.

Figure 7 shows the RDF between the carbon atoms at the left end (C_0-C_0), central part (C_{12}-C_{12}) and right end (C_{23}-C_{23}) of the PE shown in Fig. 1 (a) for each MD simulation model. In the RDF in the crystals, sharp peaks such as the delta function exist discretely up to large interatomic distances. Moreover, $g(r)$ does not converge to 1[27]. On the other hand, in the RDF obtained by this MD simulation, $g(r)$ is 0 until 3.2 Å because PE chains cannot approach each other within about 3.2 Å due to the repulsive force resulting from the overlap of electrons[27]. After that, the largest and sharp peak appeared at around 4.2 Å at the left end and right end, and around 5.2 Å at the central part of PE as shown in Fig. 1 (a). This sharp peak corresponds to the first solvation layer. Then, the second peak and third peak gradually decrease in height. Finally, $g(r)$ converges to 1. That is, the structure disappears. These are features that are not crystalline but amorphous[27].

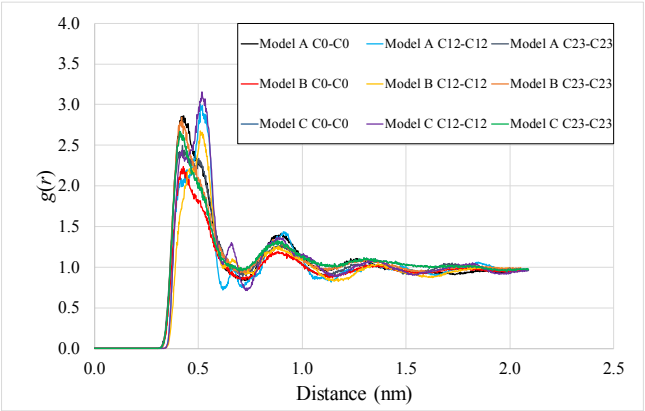

Fig. 7. RDF between the carbon atoms at the left end (C_0-C_0), central part (C_{12}-C_{12}) and right end (C_{23}-C_{23}) of the PE shown in Fig. 1 (a) for each MD simulation model

3.2 Quantum Chemical Calculation of H_2O and $5H_2O$ by DFT Figure 8 shows one water molecule (H_2O) and five water molecules ($5H_2O$) considered in this investigation[13][14]. Although water clusters should be extracted from MD simulation results, we could not successfully extract them by employing periodic boundary conditions. For $5H_2O$, a simple structure optimization based on molecular mechanics was carried out in advance. From the RDF in Fig. 6, the average distance between oxygen atoms in adjacent water molecules was found to be 0.28 nm. As a result, the distances between oxygen atoms in $5H_2O$ were set to about 0.28 nm, as shown in Table 2.

Figure 9 shows the electric dipole moments, energy levels, and molecular orbitals for H_2O and $5H_2O$. The electric dipole moment

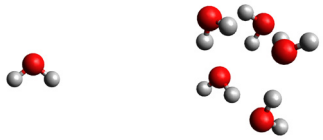

(a) H_2O (b) $5H_2O$

Fig. 8. H_2O and $5H_2O$ considered in this investigation

Table 2. Distances between oxygen atoms in $5H_2O$

Combination	Distance (nm)
O_1-O_2	0.2856
O_1-O_3	0.2.819
O_1-O_4	0.3469
O_1-O_5	0.2703
O_2-O_3	0.2752
O_2-O_4	0.2955
O_2-O_5	0.4160
O_3-O_4	0.2667
O_3-O_5	0.3983
O_4-O_5	0.2710

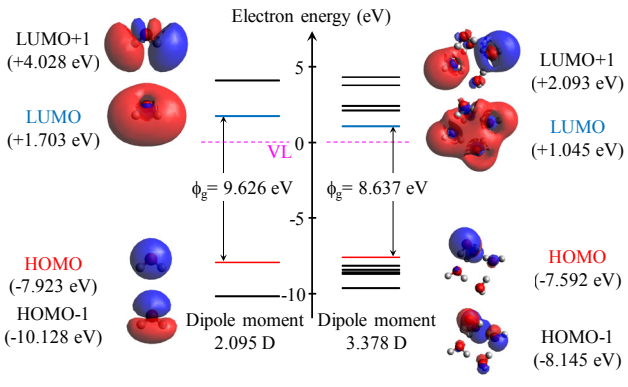

(a) H_2O (b) $5H_2O$

Fig. 9. Dipole moments, energy levels, and molecular orbitals for H_2O and $5H_2O$

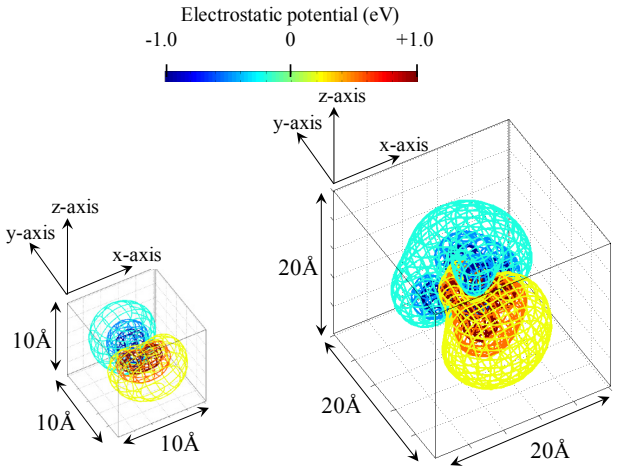

(a) H_2O (b) $5H_2O$

Fig. 10. 3D electrostatic potential distributions for H_2O and $5H_2O$

of $5H_2O$ was about 1.6 times larger than that of H_2O. Therefore, charge trapping by $5H_2O$ is easier than that by H_2O[28]. Moreover, the energy gap between the highest occupied molecular orbital (HOMO) and lowest unoccupied molecular orbital (LUMO) levels is narrow in $5H_2O$. This is due to the presence of four oxygens with high electronegativity near H_2O.

Figure 10 shows the 3D electrostatic potential distributions for H_2O and $5H_2O$. Warm colors represent positively charged regions and cold colors represent negatively charged regions. We can see that the hydrogen side is positively charged and the oxygen side is negatively charged in H_2O, as shown in Fig. 10 (a). On the other hand, in $5H_2O$, a pair of positively charged and negatively charged regions larger than those in H_2O were formed, as shown in Fig. 10 (b).

3.3 Quantum Chemical Calculation of Surfactant Alone and Surfactant in Proximity to $5H_2O$ by DFT As shown in Fig. 2, when a surfactant having a hydrophobic group and hydrophilic group is added to a hydrophobic polymer such as PE or XLPE, the surfactant forms a micelle in the amorphous region of the polymer. Therefore, it is considered that the surfactant surrounds a water cluster, stabilizing the cluster.

Here, we performed a quantum chemical calculation of the surfactant alone and the surfactant in proximity to $5H_2O$ (surfactant + $5H_2O$). That is, we calculated part of a micelle containing $5H_2O$ using DFT, as shown in Fig. 11. The closest distance between an oxygen atom of the water cluster and an oxygen atom of the surfactant is 0.2736 nm.

Figure 12 shows the electric dipole moments, energy levels, and molecular orbitals for the surfactant alone and surfactant + $5H_2O$. The electric dipole moment of surfactant + $5H_2O$ is about 2.5 times larger than that for the surfactant alone. Since water tree initiation is related to electron transfer under an electric field[1], the much larger electric dipole moment of surfactant + $5H_2O$ is considered to be more effective in electron trapping[28] and contribute more to the suppression of water tree initiation. Moreover, the energy gaps became narrower with the addition of the surfactant, particularly surfactant + $5H_2O$. While there is almost no fluctuation in the HOMO level, the LUMO level is further reduced by the addition of four water molecules. This is considered due to the effect of oxygen with high electronegativity. From the molecular orbitals,

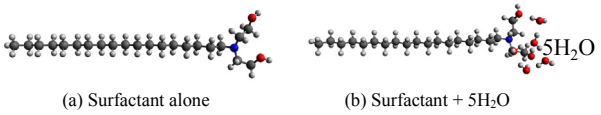

(a) Surfactant alone (b) Surfactant + $5H_2O$

Fig. 11. Surfactant alone and surfactant + $5H_2O$ as part of micelle

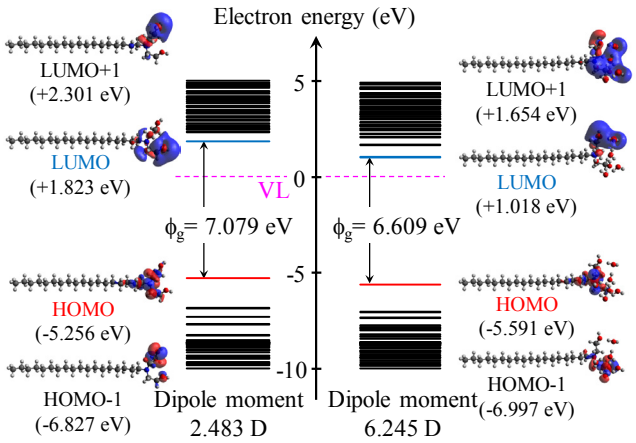

(a) Surfactant alone (b) Surfactant + $5H_2O$

Fig. 12. Dipole moments, energy levels, molecular orbitals for surfactant alone and surfactant + $5H_2O$

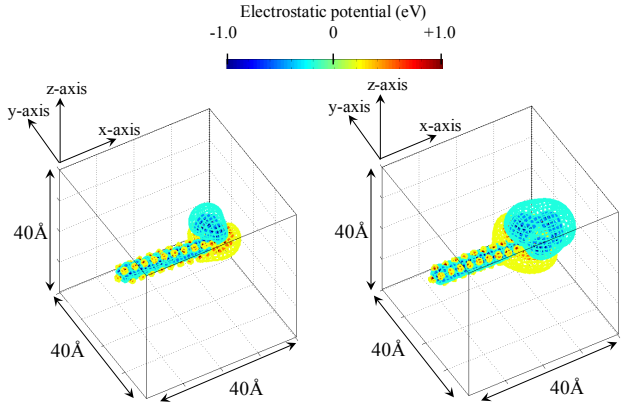

(a) Surfactant alone (b) Surfactant + $5H_2O$

Fig. 13. 3D electrostatic potential distributions for surfactant alone and surfactant + $5H_2O$

it can also be seen that the trapping sites are concentrated in the vicinity of nitrogen and oxygen, which have high electronegativity.

Figure 13 shows the 3D electrostatic potential distributions for the surfactant alone and surfactant + $5H_2O$. Since five oxygens having an electronegativity of 3.5 are located close to the surfactant in surfactant + $5H_2O$, it can be seen that the 3D electrostatic potential distribution is spread over a wide area, particularly in the hydrophilic group region of the surfactant. In contrast, there is no significant change in the hydrophobic group in the surfactant alone and surfactant + $5H_2O$. Since the surfactant contains one nitrogen and two oxygens with high electronegativity in the molecular structure, it is considered that hydrogen bonding occurs.

3.4 Effect of Surfactant on Suppression of BTT A BTT is caused by a defect such as a void or contaminant in an insulating material, as shown in Fig. 14. Moreover, there may be moisture present inside the insulating material or external moisture may

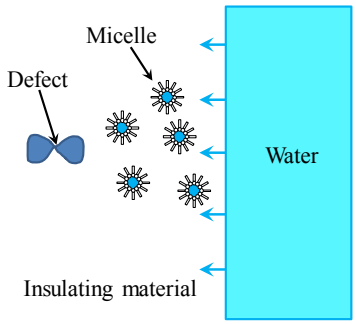

Fig. 14. Effect of surfactant on Suppression of BTT

penetrate through the insulating material to reach a defect and generate a BTT. However, when the surfactant was added, the initiation of a BTT was suppressed to less than 20% of the case without the surfactant, as shown in Fig. 3[(2)(3)].

We now consider the model shown in Fig. 14. First, moisture pre-existed inside the insulating material and/or external moisture penetrated through the insulating material form water clusters owing to hydrogen self-bonding and aggregation. Then, the amphiphilic surfactant added to the insulating material surrounds each water cluster with the hydrophilic groups oriented toward the water cluster. Hence, micelles are formed to solubilize the moisture presented in the supersaturated state in the insulating material. These micelles suppress water trees by delaying the supply of water to the defect.

4. Conclusions

In this study, we performed MD simulation and DFT quantum chemical calculations to reveal the mechanism by which water tree initiation is suppressed by amphiphilic surfactants. Our comparison of the computational results with experiments suggests that the addition of a surfactant is extremely effective in suppressing BTT. Our main findings related to the mechanism of such water tree suppression are as follows.

(1) Water molecules form a water cluster mainly by hydrogen bonding.

(2) The electric dipole moment of surfactant + $5H_2O$ is larger and the energy gap is narrower than those for the surfactant alone.

(3) We successfully modeled part of a micelle by combining a surfactant and a small water cluster.

Moreover, future tasks are as follows.

(1) The additive amount of the surfactant in which suppression of BTT was confirmed was 0.2 wt% in the experiment. However, in this MD simulation, the additive amount of the surfactant was 25 or 50 times as 4.9 wt% or 9.3 wt%, as shown in Table 1. Therefore, it is important to make a large scale simulation by increasing the length of the PE chains and to match with the actual additive amount of the surfactant.

(2) We are aware that the convergence in the basis set of 6-31g* is not suitable and this DFT calculation is sensitive to basis set. Therefore, we have a plan to use a more appropriate basis set. Although the structure optimization was performed in this DFT calculation, the self-consistent field (SCF) calculation was not set regarding the convergence condition.

(3) Although we showed that the water cluster locally has a large electric dipole moment depending on the oxygen atoms in water molecules with large electronegativity, we are now considering that this widely spread electrostatic potential distribution reduces the LUMO level of surrounding surfactant.

(4) In this study, a micelle after MD simulation could not be extracted due to periodic boundary conditions. Therefore, DFT calculation was performed by simulating a part of the micelle. In the future, we would like to extract the micelle from the final structure after MD simulation and perform DFT calculation. Thereby, we would like to seek the mechanism of initiation and propagation of BTT.

(5) We will consider the case in which an electric field is applied as well as the molecular interactions between PE, surfactants, and water molecules.

Acknowledgment

This work was supported by JSPS KAKENHI Grant Number JP18K05244.

References

(1) L. A. Dissado and J. C. Fothergill : Electric Degradation and Breakdown in Polymers, pp.75-85, Peter Peregrinus Ltd. (1992)
(2) Y. Kanemitsu, K. Takatori, Y. Sekii, and T. Goto : "Effects of Surfactant on Water Tree Generation in XLPE", *J. Inst. Electrostat. Jpn*., Vol.28, No.2, pp.127-132 (2004)
(3) Y. Sekii, N. Momose, K. Takatori, Y. Kanemitsu, and T. Goto : "Effect of Surfactant on Water Tree Generation in XLPE", Proc. 2003 ICPADM, pp.269-273 (2003)
(4) S. Iwata : "Molecular Dynamics Simulation of Effect of Glycerol Monostearate on Amorphous Polyethylene in the Presence of Water", *J. Mol. Model*., Vol.23, No.4, pp.115-1-115-7 (2017)
(5) M. Fukuda and S. Kuwajima : "Molecular-dynamics Simulation of Moisture Diffusion in Polyethylene beyond 10 ns Duration", *J. Chem. Phys*., Vol.107, No.6, pp.2149-2159 (1997)
(6) J. Mijović and H. Zhang : "Molecular Dynamics Simulation Study of Motions and Interactions of Water in a Polymer Network", *J. Phys. Chem. B*, Vol.108, No.8, pp.2557-2563 (2004)
(7) J. T. Hirvi and T. A. Pakkanen : "Molecular Dynamics Simulations of Water Droplets on Polymer Surfaces", *J. Chem. Phys*., Vol.125, p.144712 (2006)
(8) S. G. Lee, S. S. Jang, J. Kim, and G. Kim : "Distribution and Diffusion of Water in Model Epoxy Molding Compound: Molecular Dynamics Simulation Approach", *IEEE Trans. Adv. Packag*., Vol.33, No.2, pp.333-339 (2010)
(9) Q. Yin, L. Zhang, B. Jiang, Q. Yin, and K. Du : "Effect of Water in Amorphous Polyvinyl Formal: Insights from Molecular Dynamics Simulation", *J. Mol. Model*., Vol.21, pp.1-9 (2015)
(10) M. J. Frisch, G. W. Trucks, H. B. Schlegel, G. E. Scuseria, M. A. Robb, et al. : Gaussian 09, Revision D.01, Wallingford CT (2009)
(11) A. D. Becke : "Density-functional Thermochemistry. III. The Role of Exact Exchange", *J. Chem. Phys*., Vol.98, No.7, pp.5648-5652 (1993)
(12) C. Lee, W. Yang, and R. G. Parr : "Development of the Colle-Salvetti Correlation-Energy Formula into a Functional of the Electron Density", *Phys. Rev. B*, Vol.37, No.2, pp.785-789 (1988)
(13) J. K. Gregory, D. C. Clary, K. Liu, M. G. Brown, and R. J. Saykally : "The Water Dipole Moment in Water Clusters", *Science, New Series*, Vol.275, No.5301, pp.814-817 (1997)
(14) D. D. Kemp and M. S. Gordon : "An Interpretation of the Enhancement of the Water Dipole Moment Due to the Presence of Other Water Molecules", *J. Phys. Chem. A*, Vol.112, No.22, pp.4885-4894 (2008)
(15) W. L. Jorgensen, J. Chandrasekhar, J. D. Madura, R. W. Impey, and M. L. Klein : "Comparison of Simple Potential Functions for Simulating Liquid Water", *J. Chem. Phys*., Vol.79, pp.926-935 (1983)
(16) J. Wang, R. M. Wolf, J. W. Caldwell, P. A. Kollman, and D. A. Case : "Development and Testing of a General Amber Force Field", *J. Comput. Chem*., Vol.25, No.9, pp.1157-1174 (2004)
(17) T. Darden, D. York, and L. Pedersen : "Particle Mesh Ewald: An N·log(N) Method for Ewald Sums in Large Systems", *J. Chem. Phys*., Vol.98, No.12, pp.10089-10092 (1993)
(18) B. Hess, H. Bekker, H. J. C. Brendsen, and J. G. E. M. Fraaije : "Lincs: A Linear Constraint Solver for Molecular Simulation", *J. Comput. Chem*., Vol.18, No.12, pp.1463-1472 (1997)
(19) S. Nosé : "A Molecular Dynamics Method for Simulations in the Canonical Ensemble", *Mol. Phys*., Vol.52, No.2, pp.255-268 (1984)
(20) W. G. Hoover : "Canonical Dynamics: Equilibrium Phase-space Distributions", *Phys. Rev. A*, Vol.31, No.3, pp.1695-1697 (1985)

(21) M. Parrinello and A. Rahman : "Polymorphic Transitions in Single Crystals: A New Molecular Dynamics Method", *J. Appl. Phys*., Vol.52, No.12, pp.7182-7190 (1981)
(22) H. Lu, Z. Zhou, T. Hao, X. Ye, and Y. Ne : "Temperature Dependence of Structural Properties and Chain Configurational Study: a Molecular Dynamics Simulation of Polyethylene Chains", *Macromol. Theory Simul*., Vol.24, pp.335-343 (2015)
(23) A. K. Soper : "The Radial Distribution Functions of Water and Ice from 220 to 673 K and at Pressures up to 400 MPa", *Chem. Phys*., Vol.258, pp.121-137 (2000)
(24) S. Dixit, J. Crain, W. C. K. Poon, J. L. Finney, and A. K. Soper : "Molecular Segregation Observed in a Concentrated Alcohol-water Solution", *Nature*, Vol.416, pp.829-832 (2002)
(25) C. Wu and W. Wu : "Atomistic Simulation Study of Absorbed Water Influence on Structure and Properties of Crosslinked Epoxy Resin", *Polymer*, Vol.48, pp.5440-5448 (2007)
(26) M. Canales : "Influence of the Potential on the glass transition Temperature and the Structure of Amorphous Polyethylene", *Phys. Rev. E*, Vol.79, pp.051802-1-051802-10 (2009)
(27) S. Okazaki and N. Yoshii : Basics of Computer Simulation (2nd Edition), pp.165-169, Kagakudojin Co., Ltd. (2011)
(28) H. Uehara, S. Iwata, Y. Sekii, and T. Takada : "Analysis of Electrical Tree Inhibitory Effect of Antioxidants with DFT Approach", *IEEJ Trans. FM*, Vol.137, No.11, pp.600-607 (2017)

Hiroaki Uehara

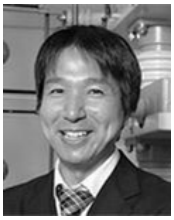

(Member) received his B.E., M.E., and Ph.D. degrees in electrical engineering from Meiji University, Tokyo, Japan, in 1995, 1997, and 2000, respectively. In 2000, he joined the staff of the College of Engineering, Kanto Gakuin University, Yokohama, Japan. In 2014, he was a visiting research scholar at The University of Connecticut for one year. He is currently a professor of the Department of Electrical and Electronic Engineering, Kanto Gakuin University, a post he has held since 2013. His research interests are insulating materials, dielectrics, and electrostatic transducers.

Shinya Iwata

(Member) received his B.E. degree from Kyoto Institute of Technology in 2005 and his M.E. and Ph.D. degrees from The University of Tokyo in 2007 and 2011, respectively. Currently, he works at Osaka Research Institute of Industrial Science and Technology as a researcher, where he is involved in the study of electrical breakdown, insulating materials, and the reliability of electrical products and systems.

Yasuo Sekii

(Life Member) received his B.Sc. degree in 1963, M.Sc. degree in 1965, and Ph.D. degree in 1976, all from The University of Tokyo, Japan. In 1965, he joined Hitachi Cable, Ltd., where he was engaged in R&D work on medium- and high-voltage AC and DC XLPE cable systems. In 1994, he moved to Chiba Institute of Technology. During 1994-2007, he was engaged in educational work while undertaking material studies on electrical and thermal degradation and on space charge generation in polymeric dielectrics. In June 2007, he was nominated to be the chairman of Japan Electric Cable Technology Center (JECTEC). He is now an advisor of Electrostatics Japan (IEJ) and a member of The Institute of Professional Engineers Japan (IPEJ).

Tatsuo Takada

(Life Member) received his B.E. degree in electrical engineering from Musashi Institute of Technology, Japan, in 1963 and his M.E. and Ph.D. degrees from Tohoku University, Japan, in 1966 and 1975, respectively. He became a lecturer, an associate professor, and a professor at Musashi Institute of Technology, in 1967, 1974, and 1987, respectively. He was a visiting scientist at MIT (USA) from 1981 to 1983. He received the Excellent Paper Award from the IEE of Japan in 1974, 1981, and 1990. In 1990, he received the Whitehead Memorial Lectureship at the IEEE CEIDP. Currently, he is involved in several research projects on space charge effects in solid dielectric materials, surface charges on thin films, and electric field measurements in liquid materials.

Yang Cao

(Non-member) received his B.S. and M.S. degrees from Tongji University, China, in 1992 and 1995, respectively, and his Ph.D. degree from The University of Connecticut in 2002. He joined the GE Global Research Center, where he worked as an electrical engineer for 11 years. He is presently an associate professor of the Department of Electrical and Computer Engineering and a director of Electrical Insulation Research Center, Institute of Materials Science at The University of Connecticut. His research interests include (1) high-electric-field phenomena and devices (2) polymeric nanostructured materials with game-changing characteristics for energy-efficient power conversion and renewable integration (3) high- voltage engineering in power and medical devices (4) grid asset management, particularly the diagnosis and prognosis of electrical degradation.